CLIMATOLOGY

An unprecedented fall drought drives Dust Bowl–like losses associated with La Niña events in US wheat production

Lina Zhang[1]†, Haidong Zhao[1]†, Nenghan Wan[1]†, Guihua Bai[2,1], M. B. Kirkham[1], John W. Nielsen-Gammon[3], Thomas J. Avenson[4], Romulo Lollato[1], Vaishali Sharda[5], Amanda Ashworth[6], Prasanna H. Gowda[7], Xiaomao Lin[1]*

Unprecedented precipitation deficits in the 2022–2023 growing season across the primary wheat-producing region in the United States caused delays in winter wheat emergence and poor crop growth. Using an integrated approach, we quantitatively unraveled a 37% reduction in wheat production as being attributable to both per–harvested acre yield loss and severe crop abandonment, reminiscent of the Dust Bowl years in the 1930s. We used random forest machine learning and game theory analytics to show that the main driver of yield loss was spring drought, whereas fall drought dominated abandonment rates. Furthermore, results revealed, across the US winter wheat belt, the La Niña phase of the El Niño Southern Oscillation (ENSO), increased abandonment rates compared to the El Niño phase. These findings underscore the necessity of simultaneously addressing crop abandonment and yield decline to stabilize wheat production amid extreme climatic conditions and provide a holistic understanding of global-scale ENSO dynamics on wheat production.

INTRODUCTION

Global wheat production faces a challenge due to the ongoing conflict between Ukraine and Russia, which has resulted in a 60% reduction in wheat trade and, consequentially, a 50% surge in wheat prices (*1*, *2*). In response to this crisis, the United States, which is recognized as the "wheat breadbasket of the world," expanded its acreage of winter wheat by 11% during 2022/2023 compared to the previous year. During this period, the US wheat heartland encountered an unforeseen and unprecedented challenge from extreme weather events. In the fall of 2022 (August to October), most states in the US winter wheat belt, including Texas, Oklahoma, Kansas, Colorado, and Nebraska, experienced a substantial precipitation deficit (Fig. 1A). This drought was particularly detrimental in Kansas, known as the "wheat state," which produces the most winter wheat in the United States (*3*). In the past 40 years (1981 to 2020), Kansas produced 359 million bushels of winter wheat per year on average, representing 23% of the US total. In 2022/2023, Kansas had a record-setting precipitation deficit dating back to 1896 (Fig. 1, A and B), with the amount of precipitation falling to 84 mm, 60% below the average between 1981 and 2010. Similar precipitation patterns and dryness rankings were observed across the entire US winter wheat belt (Fig. 1A).

Such an extreme drought affected winter wheat emergence, growth, and development, leading to the latest emergence date and the second-longest duration between planting and emergence dates in the past 40 years, which covers all available historical data (Fig. 1C). These adverse conditions dually compromised both establishment and growth. Furthermore, crop growth conditions in the first week of November 2022 were the poorest on record over the period from 1987 to 2023 (Fig. 1D). The severe drought conditions persisted into the spring of 2023 (Fig. 1, A, B, and D), further hampering growth and tillering. In Kansas, the extreme lack of precipitation in the fall and spring resulted in large portions of winter wheat to emerge in late spring rather than in early fall, shortening the period of crop development and compromising the crop's yield potential. Using combinatorial analytics, the extreme climatic conditions encountered during the 2022/2023 growing season presented a unique opportunity to understand how such events converge to influence winter wheat production.

Despite increasing research efforts, the quantitative linkages between extreme climatic change and wheat production remain ambiguous. Annual wheat production equals the product of per–harvested acre yields and harvested acreage (*4*). Both production components can theoretically be affected by climate variability and climate change. Most studies have focused on how in-season climatic factors, such as overall growing-season warming (*3*, *5*), extreme in-season temperatures (*6*, *7*), and crop-seasonal droughts (*8*, *9*), affect wheat yields. However, these studies may bear uncertain implications for estimating production variability because the far-reaching impact of climate extends beyond in-season effects and also beyond mere reductions in crop yields (*8*, *10*–*12*). Specifically, crop abandonment, defined as the difference between planted and harvested area normalized to the planted area (*13*), contributes to market volatility (*14*), global food insecurity (*15*), and greater crop insurance claims, which have been overlooked in many studies (*9*, *16*). Recent studies have explored the relationship between climate variability and crop abandonment; the results of which are typified by crop failure (*10*), a decrease in harvested ratio (the ratio of harvested area to planted area) (*17*, *18*), and changes in crop frequencies (number of

[1]Department of Agronomy, 2004 Throckmorton Plant Sciences Center, Kansas State University, Manhattan, KS 66506, USA. [2]USDA, Agricultural Research Service, Hard Winter Wheat Genetics Research Unit, Manhattan, KS 66506, USA. [3]Department of Atmospheric Sciences, Texas A&M University, College Station, TX 77843, USA. [4]Vindara Inc., Orlando, FL 32812, USA. [5]Carl and Melinda Helwig Department of Biological and Agricultural Engineering, Kansas State University, Manhattan, KS 66506, USA. [6]USDA, Agricultural Research Service, Poultry Production and Product Safety Research Unit, Fayetteville, AR 72701, USA. [7]USDA, Agricultural Research Service, Southeast Area, Stoneville, MS 38776, USA.
*Corresponding author. Email: xlin@ksu.edu
†These authors contributed equally to this work.

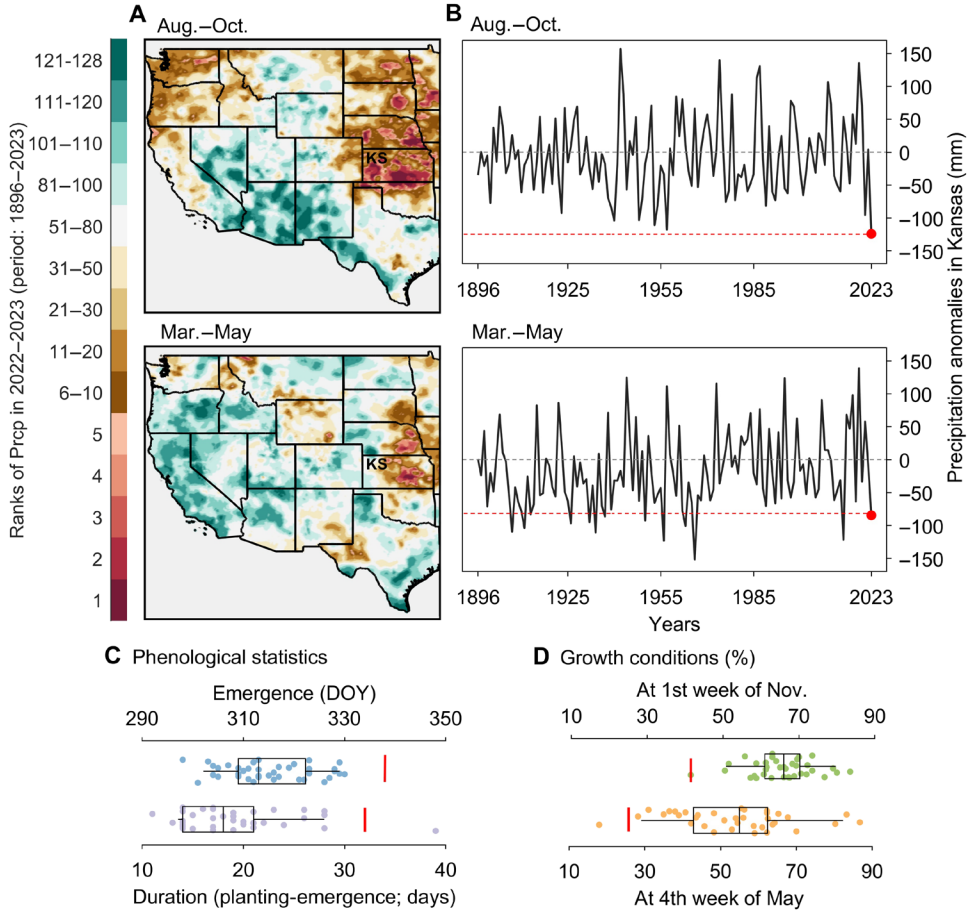

Fig. 1. Driest rankings in the United States over 128 years and the 2022–2023 winter wheat growth conditions in the wheat state of Kansas. (**A**) Rankings (driest) of accumulated precipitation (Prcp) during August to October 2022 and March to May 2023 over the past 128 years (1896 to 2023; harvested years). KS, Kansas. (**B**) Precipitation anomalies during August to October and March to May with the base period of 1981 to 2010 in Kansas. (**C**) Wheat phenological statistics of emergence date [day of year (DOY)] and duration between planting and emergence dates (days) from 1982 to 2023. (**D**) Wheat growth conditions (%) in early November (first week) and late May (fourth week) from 1987 to 2023. The boxes delimit the 25th and 75th percentiles; whiskers indicate 5th and 95th percentiles; and vertical black lines represent the 50th percentile. Red solid circles in (B) and vertical lines in (C) and (D) are for the 2023 harvest year.

crops harvested per growing season) (*19*). For example, normal temperatures or precipitation tend to increase the harvested ratio, while extreme climate conditions cause it to decrease, particularly in maize and soybean (*18*). Consequently, relying solely on per–harvested acre wheat yield as a gauge of production variability can cause uncertainty when estimating the impact of climatic variability on wheat production. To bolster global food security (*20*), it is imperative to integrate crop abandonment data into that of wheat yields when assessing production declines that are attributable to extreme weather events and climatic changes.

The occurrence of an unprecedented drought in Kansas during the 2022/2023 preseason and growing season, along with the availability of long-term data on wheat production in the state dating back to 1926, allowed us to explore the underlying mechanistic impacts of extreme climatic events on variability of wheat production. Using a random forest (RF) regression model (*21*), we provide quantitative evidence of 2023 production loss resulting from both crop abandonment and yield variation and compared that to the winter wheat production loss in both the decade of the Dust Bowl (i.e., 1930s), which was marked by the most prolonged and severe drought in modern US history (*22*, *23*), and the latest decade between 2013 and 2022. We then quantitatively disentangled the climatic drivers underlying the extreme events that caused the extreme crop abandonment and yield losses by integrating the RF model with a game theory tool (*24*). Our objectives were to understand the impact of preseasonal and in-season droughts on winter wheat production including crop abandonment and yield losses per se. Considering the widespread influence of the El Niño Southern Oscillation (ENSO) on fall precipitation in the US winter wheat belt (*25*, *26*) and high predictability of larger amplitude ENSO events (*27*, *28*), we simultaneously explored the potential connections between ENSO phases and crop abandonment that might benefit predictive crop monitoring and early warning systems (*29*) in the US winter wheat belt.

RESULTS AND DISCUSSION

Attributions of losses in winter wheat production

The observational data revealed that abandonment of winter wheat was the most severe during the 2022/2023 growing season in Kansas since the Dust Bowl era in 1930s, the exception being the year of 1951 (Fig. 2A), with an abandonment of 29%, amounting to 951,011 ha. This severity of abandonment mirrors that of the broader US winter

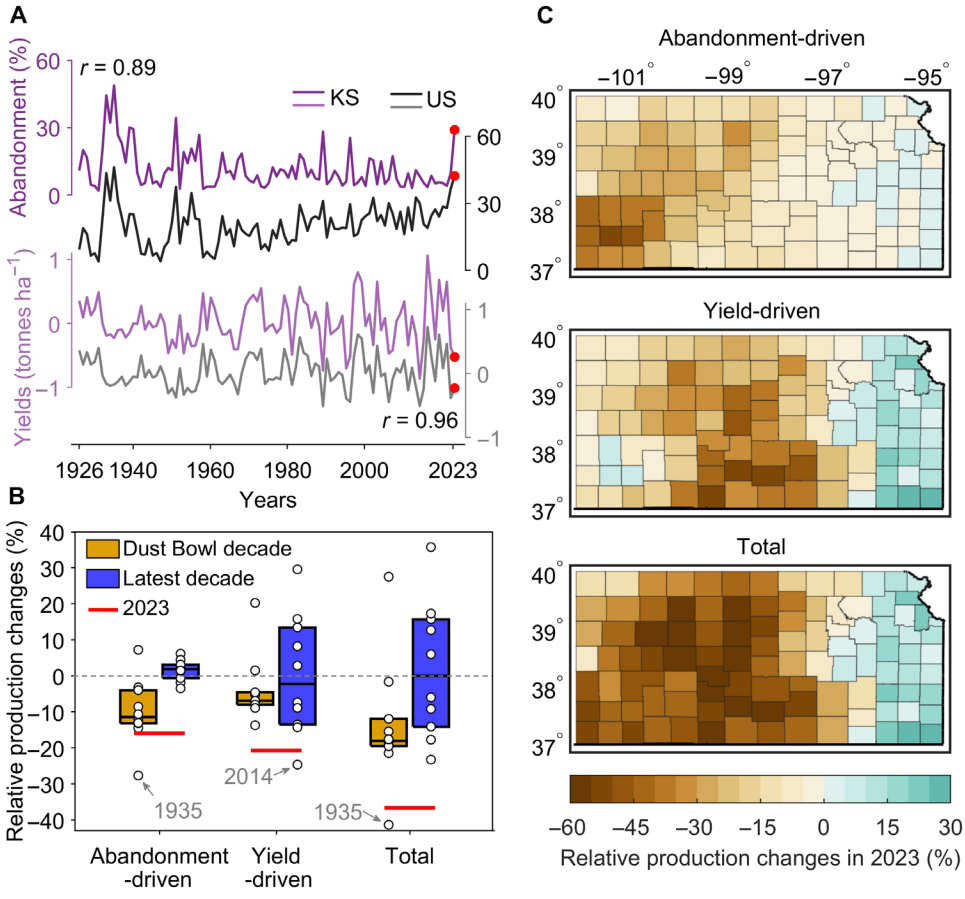

Fig. 2. Climate-driven changes in production attributed to crop abandonment and yields. (**A**) Observed time series for both crop abandonment and yield anomalies for Kansas (KS) and the United States winter wheat belt (US) including Nebraska, Colorado, Kansas, Oklahoma, and Texas. (**B**) State-level relative climate-driven production changes due to changes in abandonment and yields during the Dust Bowl decade (1931 to 1940), latest decade (2013 to 2022), and year 2023. The relative production changes are expressed as production changes relative to average production during 1981 to 2010. The boxes delimit the 25th and 75th percentiles, and the horizontal black lines represent the 50th percentile. (**C**) County-level relative production changes due to changes in abandonment and yield in the year 2023.

wheat belt, in which 2022/2023 recorded the highest level of abandonment since the middle of the Dust Bowl period (Fig. 2A). Such pronounced abandonment can be attributed to delayed emergence, adverse crop developmental conditions (Fig. 1, C and D), and diminished yield prospects. These unfavorable outcomes ultimately compelled farmers to leave their crops unharvested. Similarly, we also found a large yield loss in Kansas (Fig. 2A), with a decrease of 0.52 tonnes ha^{-1} compared to the expected yield, equivalent to 22% of expected yield (see Materials and Methods).

To quantify the impact of extreme climate during the 2022/2023 growing season on changes in abandonment and yields, we used an RF regression model. This model captured preseasonal and in-season temperature and precipitation variations as well as wheat price fluctuations (see Materials and Methods and fig. S1). We then assessed the severity of wheat production losses in the 2022/2023 growing season by comparing them with those during both the decade of the US Dust Bowl (1931 to 1940) and the most recent decade (2013 to 2022). All results were expressed as a percentage relative to the estimated average production driven by historical climate records (1981 to 2010). We found that climatic extremes during 2022/2023 resulted in a 37% loss in wheat production compared to average production during the period of 1981 to 2010. This loss was the greatest for any year throughout the most recent decade as well as that of the Dust Bowl era, with the sole exception of 1935 (Fig. 2B). The 2023 production losses were not merely due to yield decline per se, contributing to a 21% wheat production loss, but also to crop abandonment (Fig. 2B). The 16% production losses from crop abandonment in 2022/2023 are noteworthy because they are comparable to the losses caused by extreme drought during the Dust Bowl era. During that historical period, three-quarters of the average production loss of 14% was attributed to crop abandonment, while the remainder (one-quarter) was due to yield reductions per se (Fig. 2B). The role of crop abandonment in influencing crop production was also underscored in maize and soybean (*18*). Generally, crop abandonment showed a nonlinear response to temperature and precipitation. However, crop abandonment in maize and soybean is more sensitive to temperature (*18*), whereas wheat abandonment displays greater sensitivity to precipitation (fig. S2). To provide perspective, during the decade of the Dust Bowl, production losses due to changes in abandonment were much larger than losses resulting from changes in yield. In contrast, during the most recent decade, production losses caused by changes in yield were larger than those caused by changes in abandonment (Fig. 2B). In addition, we showed the comparison of observed and estimated abandonment, which augmented the credibility of our findings (fig. S3). To test the robustness of the findings, we also used two

alternative models with different sets of predictors (figs. S4A and S5A). Last, we showed the spatial distribution of climate-driven production changes in 2023, attributable to changes in crop abandonment and per–harvested acre yields (Fig. 2C). The southwest regions of Kansas exhibited the substantial production loss attributed to crop abandonment, whereas the central regions experienced severe decline in production due to yield loss (Fig. 2C), aligning with regions affected by severe spring drought (Fig. 1A). Overall, both crop abandonment and yield loss contributed to an average production decline of 50% across the central and western regions (Fig. 2C). A recent study (*17*) found that, on average, the projected future climate change by midcentury (2034 to 2065) does not significantly increase production loss through crop abandonment relative to historical averaged climate. Consequently, it was suggested that neglecting crop abandonment as a factor in future production levels would not substantially influence estimation of climate-driven production losses. However, the calibration period used in this study was relatively short and did not include most of the notable droughts of the past. Given the crucial role of crop production variability in maintaining food stability (*8*) and the impact of crop abandonment on production loss (Fig. 2, B and C), we encourage consideration of crop abandonment when estimating impact of climate variability on crop production, especially during extreme drought years. This additional measure could aid policy makers in devising effective risk management strategies and adaptation interventions.

Drivers for extreme abandonment and yield loss

We subsequently disentangled the underlying deleterious climatic conditions that led to both extreme wheat abandonment and the extreme yield loss, defined as events above the 90th percentile and below the 10th percentile, respectively, across all years (1926 to 2023) for each of the 105 counties in Kansas. The 10th and 90th percentiles were also selected for determining climatic extremes, including low and high precipitation as well as cold and warm temperature events. When we embedded a game theory tool [Shapley additive explanations (SHAP)] (*24*) into the RF regression model (Materials and Methods and Supplementary Text), our results illustrated that preseasonal fall precipitation (August to October) was the most important climate variable in relation to the extreme wheat abandonment globally, whereas spring precipitation (March to April) played a pivotal role in the extreme yield loss (Fig. 3, A and B). Specifically,

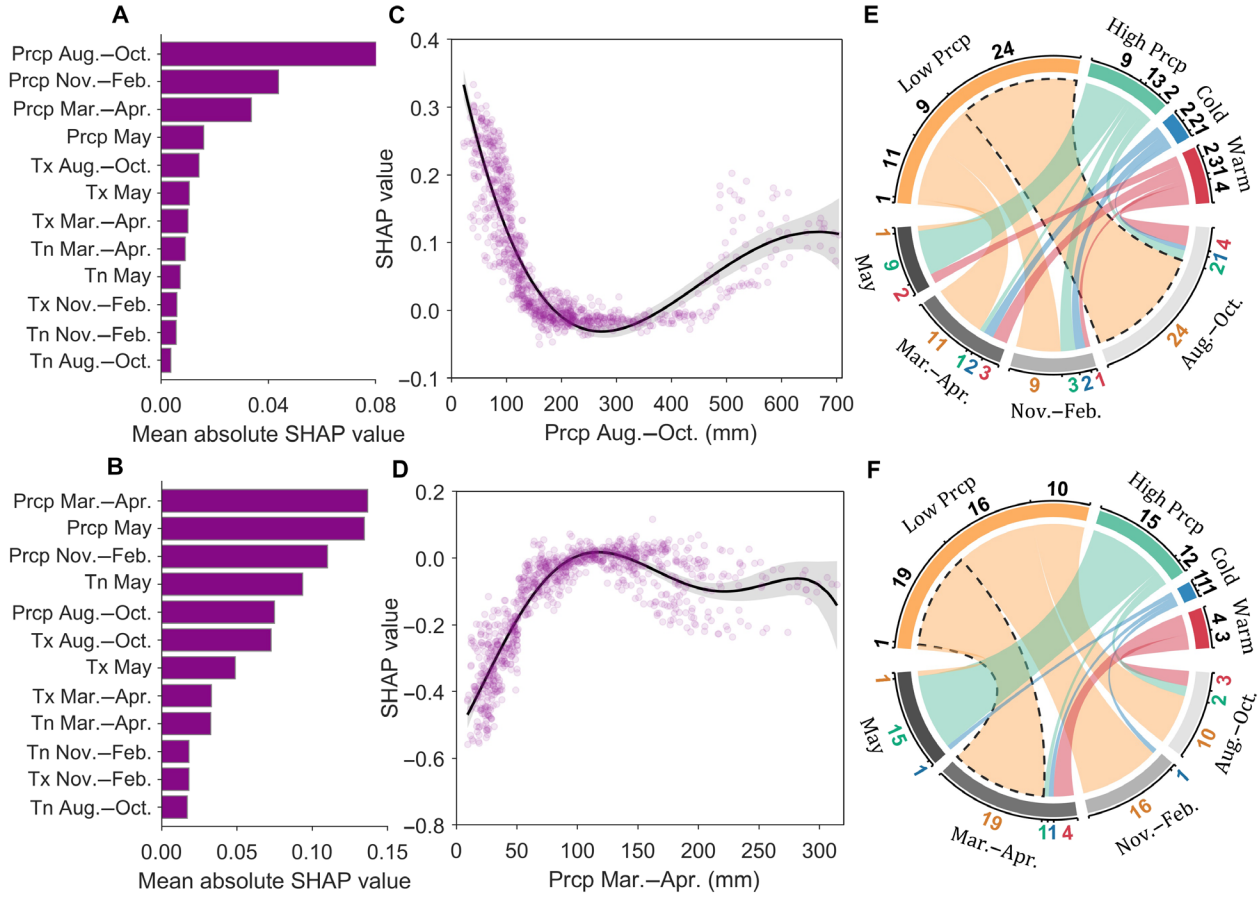

Fig. 3. Climate drivers of extreme abandonment and extreme yield losses. (**A**) Importance (SHAP values) of climate variables during county-years of extreme abandonment ordered from greatest to least important. (**B**) Same as (A) but during county-years of extreme yield losses. (**C**) Influence of the precipitation (Prcp) during August to October (the most important variable on extreme abandonment). Circles are sample points for county-years of extreme abandonment. Black solid line is the fitted line, and shaded area around the solid line indicates 95% confidence interval. (**D**) Same as (C) but for influence of the precipitation during March to April (the most important variable on extreme yield losses). (**E**) The width (or numbers) of the chords indicates the fractions (%) of area that suffered extreme abandonment (total 75%) driven by primary climatic extremes (low and high precipitation and cold and warm temperatures) across Kansas from 1926 to 2023. Black dashed lines highlight the most primary climatic drivers. (**F**) Same as (E) but for fraction of the area that suffered extreme yield losses (total 74%).

abandonment rates exhibited a nonlinear response to fall precipitation, especially with deficits in fall precipitation correlating to higher abandonment rates (Fig. 3C). Conversely, spring precipitation deficits were associated with the occurrence of extreme yield loss (Fig. 3D). Last, we estimated the primary climate extreme driving severe abandonment and yield loss (fig. S6 and Supplementary Text). We found that climatic extremes were the primary factors in 75 and 74% of the areas that suffered severe abandonment and yield loss across Kansas from 1926 to 2023, respectively (Fig. 3, E and F). In addition, extremely low wheat prices (<10th percentile) accounted for 6.6% of the areas that experienced severe abandonment (fig. S6). We also found that drought in March to April was the primary factor in 19% of the areas of extreme yield losses (Fig. 3F). In contrast, abandonment was predominantly triggered by fall drought events, which contributed 24% to the severe abandonment area (Fig. 3E). Moreover, the excessive precipitation in May was associated with both extreme abandonment and yield loss, which is consistent with another study estimating climate-driven crop failure in the United States (*10*). These results were consistent with those based on two alternative models (figs. S4, B and C, and S5, B and C). The role of spring and early summer drought, which is critical for grain filling and yield formulation, has been extensively studied (*3*, *30*). We also found that droughts in the fall and winter largely contributed to extreme yield losses (Fig. 3F), consistent with another study (*31*). To our knowledge, however, the significance of fall drought as a catalyst for crop abandonment and subsequent production losses has not previously been highlighted. The impact of fall drought on wheat abandonment can be attributed to the fact that winter wheat is usually sown in autumn, relying on sufficient soil moisture during this period to establish seedlings with robust root systems that promote healthy growth. Our study substantiates the relationship between fall precipitation and both observed abandonment rates (fig. S7) and crop growing conditions at the end of the fall season (fig. S8).

ENSO teleconnections on winter wheat abandonment

Droughts in the US winter wheat belt have been confirmed to be influenced by the ENSO (*25*, *32*, *33*). During La Niña, which is characterized by cooler-than-normal sea surface temperatures (SSTs) in the eastern tropical Pacific, the US winter wheat belt tends to experience fall droughts (fig. S9), as was observed in the 1930s (*26*), potentially leading to crop abandonment. To explore the direct role of ENSO in explaining variations in crop abandonment, we calculated average anomalies of crop abandonment during both El Niño and La Niña phases (see Materials and Methods) (*34*, *35*). The statistical significance of the changes was determined by bootstrapping (n = 10,000) at a 95% confidence level. We found that crop abandonment was reduced during the El Niño phase across five winter wheat production states, with a significant decrease of 3% on average, ranging from 0.6 to 5.2% (Fig. 4A). This is expected because El Niño causes the jet stream to shift southward and extend eastward over southern United States. Conversely, during the La Niña phase, crop abandonment showed a notable increase of 5%, with ranges between 2.7 and 8.6% across states (Fig. 4A). Except for Nebraska, all states exhibited a notable increase in crop abandonment during the transition from El Niño to La Niña phase, with variations observed among states (Fig. 4B). In Kansas, the transition from El Niño to La Niña phase intensified crop abandonment by 9%, equivalent to the US level (Fig. 4B). We further explored the impacts of ENSO on crop abandonment at a county level across the US winter wheat belt and found that the La Niña phase significantly increased abandonment rates compared to the El Niño phase. The main regions affected by abandonment were in western Kansas, the panhandle areas of Oklahoma, and western Texas (Fig. 4C), which mirrored the footprint of Dust Bowl–affected regions in the 1930s (*7*, *23*).

Several studies have suggested the urgent need for a twofold increase in global crop production by 2050 in response to the growing population (*36*). Whether or not we are on track to double production by 2050 depends on sustainable and improved harvestable crop yields (*37*, *38*). Future production variability in projected climatic scenarios will be influenced by the often-overlooked changes in crop abandonment (Fig. 2), an especially noteworthy risk given the threats of climatic extremes (*39*, *40*).

In sum, our analyses revealed climatic drivers underlying crop abandonment and the influence of ENSO dynamics on winter wheat production. La Niña events increased the probability of drought events before planting (preseason) of winter wheat in the US Great Plains. The extremely dry climate in 2022–2023 that followed nearly three consecutive years of La Niña events provided an opportunity to determine the underlying drivers of climatic extremes that negatively affect wheat production. Our study emphasized both the overlooked role of crop abandonment on wheat production in the US winter wheat belt and the underlying climate extremes that drive the two components of production loss—abandonment and yield loss. Recognizing that preseason droughts primarily drive crop abandonment, farmers could adapt their strategies, such as adjusting planting schedules, selecting drought-resistant cultivars, or investing in water management strategies tailored for the preseason. These measures can mitigate the effects of these droughts and stabilize crop production. It is also important for policy makers to design and promote initiatives encouraging drought mitigation practices for stable food production.

MATERIALS AND METHODS

Data

County- and state-level winter wheat yield, harvested area, and planted area data were retrieved from the US Department of Agriculture, National Agricultural Statistics Service (USDA-NASS) for all counties in Kansas and spanning the years 1926 to 2023. State-level planting and emergence dates (1982 to 2023) and weekly crop condition reports (1987 to 2023) were also collected from the USDA-NASS, which are the longest length available for the data. Climatic data (precipitation, maximum temperature, and minimum temperature) from 1895 to 2023 were obtained from the monthly US Historical Climatology Network maintained by the National Oceanic and Atmospheric Administration (NOAA). The monthly SSTs were taken from the Met Office Harley Centre Observations datasets (HadISST v1.1) (*41*) for calculating ENSO signals based on the Niño3.4 region (5°N–5°S, 120°W–170°W). Crop conditions were evaluated using an index ranging from 0 to 100% (*42*). The growing season of winter wheat is generally considered to be September to May in Kansas (*7*), but we used climatic data starting in August to capture the effects of climate in the month preceding planting. We divided the growing season into fall (August to October), winter (November to February), spring (March to April), and early summer (May; wheat grain filling).

Modeling

On the basis of the conceptual framework (Supplementary Text), we ran two separate RF models to estimate two components of production losses due to climate variation: the abandonment fraction and

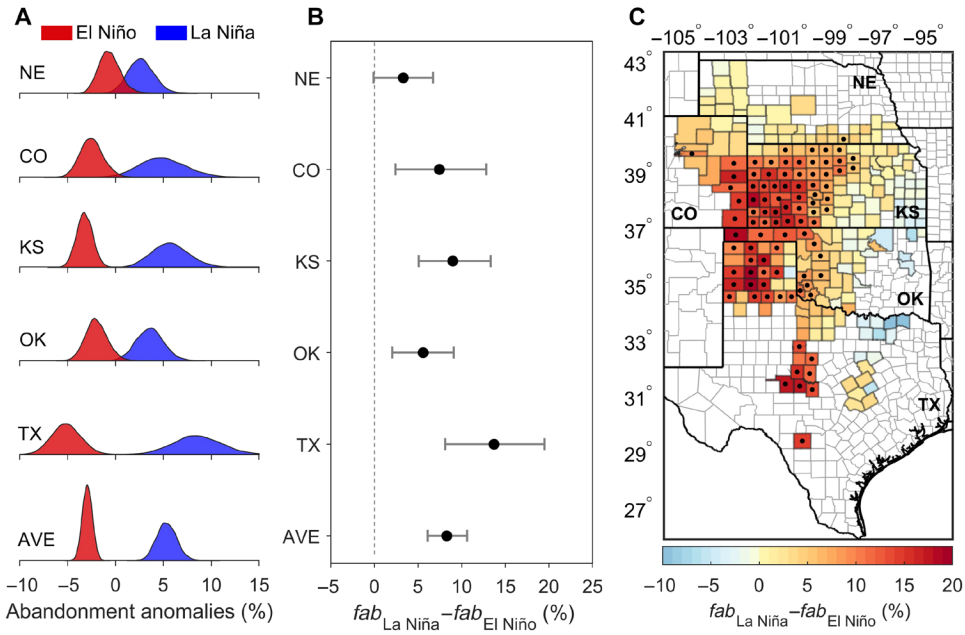

Fig. 4. Impacts of ENSO phases on crop abandonment anomalies. (**A**) Distributions of state-level crop abandonment (*fab*) anomalies during El Niño (red) and La Niña (blue) phases in Nebraska (NE), Colorado (CO), Kansas (KS), Oklahoma (OK), and Texas (TX). Negative and positive values indicate ENSO phases decreased and increased crop abandonment, respectively. (**B**) Changes in *fab* during the transition from El Niño to La Niña phase. Black solid circles indicate averages, and error bars represent 2.5th and 97.5th percentiles. (**C**) County-level changes in crop abandonment between La Niña and El Niño phases. Black dots indicate statistical significance at a 95% confidence level. Note that the state-level impact of the ENSO phase on crop abandonment was estimated by using state-level data shown in table S2.

yield anomalies. Abandonment fraction here is expressed as $\frac{PA-HA}{PA}$, where *PA* and *HA* are the planted and harvested areas, respectively, in hectares. This expression enables meaningful comparisons across different county-years with varying planted areas. Yield anomalies were calculated as the difference between actual yields and expected yields, with expected yields representing the historical yield trends driven by agricultural advancements in breeding technology and crop management. Thus, a negative anomaly suggests that yields are less than expected, possibly due to an adverse climate, disease, or other challenges. Yield trends were evaluated using a locally weighted smoothing regression (*43*) with the standard setting of the function (fig. S10).

The RF specifications for abandonment fraction (*fab*) and yield anomaly (ΔY) are

$$fab_{c,y} = F(clm_{c,y}, price_y) + \varepsilon_{c,y} \quad (1)$$

$$\Delta Y_{c,y} = F(clm_{c,y}) + \varepsilon_{c,y} \quad (2)$$

where F is an RF function; $clm_{c,y}$ represents the climate variables including monthly or seasonal maximum temperature (Tx, °C) and minimum temperature (Tn, °C), and accumulated precipitation (Prcp, mm) during four growth periods for county "*c*" and year "*y*"; the detrended $price_y$ (inflation-adjusted based on the consumer price index of 2023) by the locally weighted smoothing regression was incorporated into the "*fab*" model to isolate the effects of price changes on farmers' decisions to abandon their crop; and $\varepsilon_{c,y}$ refers to the error. The number of trees and the number of variables tested at each node in the RF model are two key parameters (*21*). To determine the optimum parameters for each model above, we partitioned 90% of data to the train model and the remaining 10% of data to the test model. Model predicted performance was estimated by the coefficient of determination (R^2) and root mean square error (table S1 and fig. S1).

The RF results were used to estimate climate-driven production changes from yield and abandonment relative to the historical climate-driven average production over 1981 to 2010 ($\widehat{P_{base}}$) for the Dust Bowl decade (1931 to 1940), the latest decade (2013 to 2022), and the year 2023. The wheat price in the *fab* model was fixed to the average of 1981 to 2010 to isolate price effects. State-level production change (%P') in specific years of interest (e.g., 2023) was defined as a relative change with respect to $\widehat{P_{base}}$

$$\%P'_y = \frac{\Delta P_{fab,y} + \Delta P_{Y,y}}{\widehat{P_{base}}} \times 100 \quad (3)$$

where $\Delta P_{fab,y}$ and $\Delta P_{Y,y}$ are defined as climate-caused production changes from the changes in abandonment and in yields, respectively. Details of calculations for these two components are given in the Supplementary Text.

The climate driver of extreme abandonment or yield loss

Next, we integrated a game theory (SHAP) (*24*) into the RF models (Eqs. 1 and 2) to assess the critical climate drivers in extreme wheat abandonment and yield loss. Specifically, for all instances of extreme wheat abandonment and yield loss events, we used SHAP values to infer variable importance in the model outcome (*44*). SHAP values are a machine learning analog of partial regression, quantifying the relative importance of each variable on the outcome while considering all other variables in the model. The overall variable importance was

determined by the mean of the absolute value of the SHAP values, and the marginal effect of variable with the highest relative importance was visualized by plotting the covariate versus the corresponding SHAP value for each observation. Last, we assessed the critical extreme climate drivers in severe wheat abandonment and yield losses (Supplementary Text).

Robustness checks

To ensure the robustness of our analysis, we conducted two checks on the RF models with two additional sets of predictors. First, we substituted the precipitation in our preferred RF models with the mean monthly Palmer's Z-index sourced from the NOAA. The Z-index is a measure of the monthly moisture anomaly and reflects the departure of moisture conditions from normal moisture conditions in a particular month (*45*). Second, because of the high collinearity between mean temperature and extreme hot/cold days, we tested the fraction of warm days and cold days to replace the mean Tx and Tn in our models to evaluate our results (figs. S4 and S5 and table S1). Specifically, the daily maximum and minimum temperatures were taken from the daily Global Historical Climatology Network (GHCN) and interpolated with a Delaunay triangulation method (*46*) to the centroid of each county in Kansas. Then, we defined the fraction of warm/cold days by calculating the number of days with maximum/minimum temperatures above/below the local historical 90th/10th percentile divided by the duration of growing season.

Crop abandonment statistics during ENSO phases

To spatially analyze the impacts of ENSO oscillation on crop abandonment, we broadened our coverage to encompass the entire US winter wheat belt, including Nebraska, Colorado, Kansas, Oklahoma, and Texas. Data for planted and harvested areas at the county and state levels were collected from the USDA-NASS, and corresponding available years are provided in table S2. We selected counties with both more than 50 available years of data and an average harvested area (1981 to 2010) exceeding 5000 ha. We next calculated averages of detrended crop abandonment (*fab*) based on locally weighted smoothing regression (i.e., fig. S11) at specific ENSO phases

$$fab_{\text{El Niño},c} = \frac{\sum_{y=\text{initial}}^{2023} fab'_{c,y}}{N_{\text{El Niño}}};\quad \text{ENSO} > 0.5$$
$$fab_{\text{La Niña},c} = \frac{\sum_{y=\text{initial}}^{2023} fab'_{c,y}}{N_{\text{La Niña}}};\ \text{ENSO} < -0.5 \tag{4}$$

where $fab_{\text{El Niño},c}$ and $fab_{\text{La Niña},c}$ are the average crop abandonment anomalies in El Niño and La Niña years (y) for county c, respectively; N refers to year numbers of the specific ENSO phase; and fab' refers to detrended crop abandonment anomalies. The ENSO signal here is defined as a 3-month running mean after being linearly detrended and standardized. We specifically calculated the average ENSO signals for Texas and Oklahoma from December to February and those for Kansas, Colorado, and Nebraska from August to October. These selected periods align with the planting dates of winter wheat (*7*). On the basis of the same method, the state-level $fab_{\text{El Niño}}$ and $fab_{\text{La Niña}}$ were also calculated. We then calculated the difference of *fab* anomalies between La Niña and El Niño phases as

$$\Delta fab_c = fab_{\text{La Niña},c} - fab_{\text{El Niño},c} \tag{5}$$

Positive (or negative) values of Δfab indicate that the La Niña phase exacerbates (or mitigates) crop abandonment relative to the El Niño phase. The statistical significance for changes in Δfab_c were determined through a bootstrapping sampling procedure ($n = 10{,}000$) at a 95% confidence level. The mean change for each bootstrap sample was calculated, and the change was considered statistically significant if, in a two-sided t test, over 95% of the sample means were consistently smaller or larger than zero.

Supplementary Materials

This PDF file includes:

Supplementary Text
Figs. S1 to S12
Tables S1 and S2

REFERENCES AND NOTES

1. F. Lin, X. Li, N. Jia, F. Feng, H. Huang, J. Huang, S. Fan, P. Ciais, X.-P. Song, The impact of Russia-Ukraine conflict on global food security. *Glob. Food Secur.* **36**, 100661 (2023).
2. K. A. Mottaleb, G. Kruseman, S. Snapp, Potential impacts of Ukraine-Russia armed conflict on global wheat food security: A quantitative exploration. *Glob. Food Secur.* **35**, 100659 (2022).
3. J. Tack, A. Barkley, L. L. Nalley, Effect of warming temperatures on US wheat yields. *Proc. Natl. Acad. Sci. U.S.A.* **112**, 6931–6936 (2015).
4. T. Iizumi, N. Ramankutty, How do weather and climate influence cropping area and intensity? *Glob. Food Secur.* **4**, 46–50 (2015).
5. C. Zhao, B. Liu, S. Piao, X. Wang, D. B. Lobell, Y. Huang, M. Huang, Y. Yao, S. Bassu, P. Ciais, Temperature increase reduces global yields of major crops in four independent estimates. *Proc. Natl. Acad. Sci. U.S.A.* **114**, 9326–9331 (2017).
6. S. Asseng, I. Foster, N. C. Turner, The impact of temperature variability on wheat yields. *Glob. Chang. Biol.* **17**, 997–1012 (2011).
7. H. Zhao, L. Zhang, M. Kirkham, S. M. Welch, J. W. Nielsen-Gammon, G. Bai, J. Luo, D. A. Andresen, C. W. Rice, N. Wan, U.S. winter wheat yield loss attributed to compound hot-dry-windy events. *Nat. Commun.* **13**, 7233 (2022).
8. C. Lesk, P. Rowhani, N. Ramankutty, Influence of extreme weather disasters on global crop production. *Nature* **529**, 84–87 (2016).
9. M. Glotter, J. Elliott, Simulating US agriculture in a modern Dust Bowl drought. *Nat. Plants* **3**, 16193 (2016).
10. S. M. Kim, R. Mendelsohn, Climate change to increase crop failure in U.S. *Environ. Res. Lett.* **18**, 014014 (2023).
11. D. Wei, J. A. Gephart, T. Iizumi, N. Ramankutty, K. F. Davis, Key role of planted and harvested area fluctuations in US crop production shocks. *Nat. Sustain.* **6**, 1177–1185 (2023).
12. F. Schierhorn, D. Müller, A. V. Prishchepov, M. Faramarzi, A. Balmann, The potential of Russia to increase its wheat production through cropland expansion and intensification. *Glob. Food Secur.* **3**, 133–141 (2014).
13. R. P. Lollato, G. P. Bavia, V. Perin, M. Knapp, E. A. Santos, A. Patrignani, E. D. DeWolf, Climate-risk assessment for winter wheat using long-term weather data. *J. Agron.* **112**, 2132–2151 (2020).
14. I. Hashmiu, O. Agbenyega, E. Dawoe, Determinants of crop choice decisions under risk: A case study on the revival of cocoa farming in the Forest-Savannah transition zone of Ghana. *Land Use Policy* **114**, 105958 (2022).
15. Q. Zheng, T. Ha, A. V. Prishchepov, Y. Zeng, H. Yin, L. P. Koh, The neglected role of abandoned cropland in supporting both food security and climate change mitigation. *Nat. Commun.* **14**, 6083 (2023).
16. T. Iizumi, I.-E. A. Ali-Babiker, M. Tsubo, I. S. Tahir, Y. Kurosaki, W. Kim, Y. S. Gorafi, A. A. Idris, H. Tsujimoto, Rising temperatures and increasing demand challenge wheat supply in Sudan. *Nat. Food* **2**, 19–27 (2021).
17. O. S. Obembe, N. P. Hendricks, J. Tack, Decreased wheat production in the USA from climate change driven by yield losses rather than crop abandonment. *PLOS ONE* **16**, e0252067 (2021).
18. X. Cui, Beyond yield response: Weather shocks and crop abandonment. *J. Assoc. Environ. Resour. Econ.* **7**, 901–932 (2020).
19. A. S. Cohn, L. K. VanWey, S. A. Spera, J. F. Mustard, Cropping frequency and area response to climate variability can exceed yield response. *Nat. Clim. Chang.* **6**, 601–604 (2016).

20. J. R. Porter, L. Xie, A. J. Challinor, K. Cochrane, S. M. Howden, M. M. Iqbal, D. B. Lobell, M. I. Travasso, Food security and food production systems, in *Climate Change 2014: Impacts, Adaptation, and Vulnerability. Part A: Global and Sectoral Aspects. Contribution of Working Group II to the Fifth Assessment Report of the Intergovernmental Panel on Climate Change* (Cambridge Univ. Press, 2014), pp. 485–533.
21. L. Breiman, Random forests. *Mach. Learn.* **45**, 5–32 (2001).
22. J. Romm, The next dust bowl. *Nature* **478**, 450–451 (2011).
23. S. D. Schubert, M. J. Suarez, P. J. Pegion, R. D. Koster, J. T. Bacmeister, On the cause of the 1930s dust bowl. *Science* **303**, 1855–1859 (2004).
24. L. S. Shapley, "A value for n-person games", in *Contributions to the Theory of Games* (Princeton Univ. Press, 1953).
25. A. Dai, Drought under global warming: A review. *Wiley Interdiscip. Rev. Clim. Change* **2**, 45–65 (2011).
26. B. I. Cook, R. L. Miller, R. Seager, Amplification of the North American "Dust Bowl" drought through human-induced land degradation. *Proc. Natl. Acad. Sci. U.S.A.* **106**, 4997–5001 (2009).
27. A. Kumar, M. Chen, Understanding skill of seasonal mean precipitation prediction over California during boreal winter and role of predictability limits. *J. Climate* **33**, 6141–6163 (2020).
28. M. L. L'Heureux, A. F. Levine, M. Newman, C. Ganter, J. J. Luo, M. K. Tippett, T. N. Stockdale, "ENSO prediction", in *El Niño Southern Oscillation in a Changing Climate* (American Geophysical Union, 2020), pp. 227–246.
29. F. Rembold, M. Meroni, F. Urbano, G. Csak, H. Kerdiles, A. Perez-Hoyos, G. Lemoine, O. Leo, T. Negre, ASAP: A new global early warning system to detect anomaly hot spots of agricultural production for food security analysis. *Agr. Syst.* **168**, 247–257 (2019).
30. E. Dickin, D. Wright, The effects of winter waterlogging and summer drought on the growth and yield of winter wheat (Triticum aestivum L.). *Eur. J. Agron.* **28**, 234–244 (2008).
31. W. Anderson, R. Seager, W. Baethgen, M. Cane, Life cycles of agriculturally relevant ENSO teleconnections in North and South America. *Int. J. Climatol.* **37**, 3297–3318 (2017).
32. S. D. Schubert, M. J. Suarez, P. J. Pegion, R. D. Koster, J. T. Bacmeister, Causes of long-term drought in the U.S. Great Plains. *J. Climate* **17**, 485–503 (2004).
33. K. C. Mo, Interdecadal modulation of the impact of ENSO on precipitation and temperature over the United States. *J. Climate* **23**, 3639–3656 (2010).
34. T. Iizumi, J.-J. Luo, A. J. Challinor, G. Sakurai, M. Yokozawa, H. Sakuma, M. E. Brown, T. Yamagata, Impacts of El Niño Southern Oscillation on the global yields of major crops. *Nat. Commun.* **5**, 3712 (2014).
35. C. B. d'Amour, L. Wenz, M. Kalkuhl, J. C. Steckel, F. Creutzig, Teleconnected food supply shocks. *Environ. Res. Lett.* **11**, 035007 (2016).
36. D. K. Ray, N. D. Mueller, P. C. West, J. A. Foley, Yield trends are insufficient to double global crop production by 2050. *PLOS ONE* **8**, e66428 (2013).
37. T. Fischer, D. Byerlee, G. Edmeades, *Crop Yields and Global Food Security* (ACIAR, 2014), pp. 8–11.
38. S. P. Long, A. Marshall-Colon, X.-G. Zhu, Meeting the global food demand of the future by engineering crop photosynthesis and yield potential. *Cell* **161**, 56–66 (2015).
39. S. Zhou, B. Yu, Y. Zhang, Global concurrent climate extremes exacerbated by anthropogenic climate change. *Sci. Adv.* **9**, eabo1638 (2023).
40. K. P. Tripathy, S. Mukherjee, A. K. Mishra, M. E. Mann, A. P. Williams, Climate change will accelerate the high-end risk of compound drought and heatwave events. *Proc. Natl. Acad. Sci. U.S.A.* **120**, e2219825120 (2023).
41. N. Rayner, D. E. Parker, E. Horton, C. K. Folland, L. V. Alexander, D. Rowell, E. C. Kent, A. Kaplan, Global analyses of sea surface temperature, sea ice, and night marine air temperature since the late nineteenth century. *J. Geophys. Res. Atmos.* **108**, https://doi.org/10.1029/2002JD002670 (2003).
42. R. Bain, T. R. Fortenbery, Impact of crop condition reports on national and local wheat markets. *J. Agric. Appl. Econ.* **49**, 97–119 (2017).
43. W. S. Cleveland, S. J. Devlin, Locally weighted regression: An approach to regression analysis by local fitting. *J. Am. Stat. Assoc.* **83**, 596–610 (1988).
44. S. M. Lundberg, G. Erion, H. Chen, A. DeGrave, J. M. Prutkin, B. Nair, R. Katz, J. Himmelfarb, N. Bansal, S.-I. Lee, From local explanations to global understanding with explainable AI for trees. *Nat. Mach. Intell.* **2**, 56–67 (2020).
45. R. R. Heim Jr., A review of twentieth-century drought indices used in the United States. *Bull. Am. Meteorol. Soc.* **83**, 1149–1166 (2002).
46. C. B. Barber, D. P. Dobkin, H. Huhdanpaa, The quickhull algorithm for convex hulls. *ACM Trans. Math. Softw.* **22**, 469–483 (1996).

Acknowledgments: We thank R. Aiken for discussions and review of the manuscript. We are also grateful to G. Sassenrath for insights into the wheat farmer's planted areas and practices. This manuscript is contribution no. 25-007-J from the Kansas Agricultural Experiment Station. **Funding:** This work was supported by the US National Science Foundation Convergence Accelerator (nos. E2061825 and FAIN:2345039) (X.L.), USDA Agricultural Research Service (A22-0103-001) (X.L.), and National Research Initiative Competitive Grant 2022-68013-36439 from the USDA National Institute of Food and Agriculture (G.B.). **Author contributions:** Conceptualization: X.L. and T.J.A. Analysis: L.Z. and H.Z. Investigation: X.L., J.W.N.-G., L.Z., H.Z., and N.W. Collection of raw data: L.Z., H.Z., and N.W. Supervision: X.L., G.B., M.B.K., and J.W.N.-G. Writing—original draft: L.Z., H.Z., N.W., and X.L. Writing—review and editing: all coauthors. **Competing interests:** The authors declare that they have no competing interests. **Data and materials availability:** Crop data are obtained from the USDA-NASS (https://quickstats.nass.usda.gov/); monthly climate data are from the NOAA (https://ncei.noaa.gov/pub/data/cirs/climdiv/); the daily maximum and minimum temperatures were taken from the daily GHCN (https://ncei.noaa.gov/data/global-historical-climatology-network-daily/); and ENSO signals based on the Niño3.4 region are obtained from (https://psl.noaa.gov/gcos_wgsp/Timeseries/Nino34/). Data analysis was carried out using MATLAB R2023a. The code developed to generate the figures is available at https://doi.org/10.6084/m9.figshare.24233152.v1. All data needed to evaluate the conclusions in the paper are present in the paper and/or the Supplementary Materials.

Submitted 16 February 2024
Accepted 26 June 2024
Published 31 July 2024
10.1126/sciadv.ado6864